Mon. Not. R. Astron. Soc. **395,** 1257–1264 (2009) doi:10.1111/j.1365-2966.2009.14622.x

Determining the spin of two stellar-mass black holes from disc reflection signatures

R. C. Reis,[1⋆] A. C. Fabian,[1] R. R. Ross[2] and J. M. Miller[3]

[1] *Institute of Astronomy, Madingley Road, Cambridge, CB3 0HA*
[2] *Physics Department, College of the Holy Cross, Worcester, MA 01610, USA*
[3] *Department of Astronomy, University of Michigan, 500 Church Street, Ann Arbor, MI 48109, USA*

Accepted 2009 February 10. Received 2009 February 10; in original form 2008 July 30

ABSTRACT

We present measurements of the dimensionless spin parameters and inner-disc inclination of two stellar-mass black holes. The spin parameter of SWIFT J1753.5−0127 and GRO J1655−40 is estimated by modelling the strong reflection signatures present in their *XMM–Newton* observations. Using a newly developed, self-consistent reflection model which includes the blackbody radiation of the disc as well as the effect of Comptonization, blurred with a relativistic line function, we infer the spin parameter of SWIFT J1753.5−0127 to be $0.76^{+0.11}_{-0.15}$. The inclination of this system is estimated at $55^{\circ}{}^{+2}_{-7}$. For GRO J1655−40, we find that the disc is significantly misaligned to the orbital plane, with an innermost inclination of $30^{\circ}{}^{+5}_{-10}$. Allowing the inclination to be a free parameter, we find a lower limit for the spin of 0.90, this value increases to that of a maximal rotating black hole when the inclination is set to that of the orbital plane of J1655−40. Our technique is independent of the black hole mass and distance, uncertainties in which are among the main contributors to the spin uncertainty in previous works.

Key words: accretion, accretion discs – black hole physics – X-rays: individual: J1753.5−0127, J1655−40.

1 INTRODUCTION

Black holes can be described by two observable parameters, mass and spin. To date, there are over 20 stellar-mass black holes with dynamically constrained mass (for a review, see McClintock & Remillard 2006); however, for just a handful of these systems do we have any measurements of their spin.

Shafee et al. (2006) and McClintock et al. (2006) have reported values of the dimensionless spin parameter, a, for 4U 1543−47 of 0.7–0.85, GRO J1655−40 of 0.65–0.75 and GRS 1915+105 of 0.98−1. More recently, Liu et al. (2008) reported a value of 0.77 ± 0.05 for M33 X-7. Their approach relies on modelling the thermal continuum seen in the thermal X-ray spectra and requires sources to be selected in the high-soft state (for a review on spectral states, see McClintock & Remillard 2006). Any power-law emission is then minimal and the spectrum resembles a quasi-blackbody continuum. Furthermore, precise measurements of the mass and distance to the black hole, as well as the inclination of the system, are essential.

We have recently reported precise measurements of the spin parameter in GX 339−4 (Miller et al. 2008a; Reis et al. 2008) using the reflection signatures in the spectrum. These reflection features arise due to reprocessing of hard X-ray by the cooler accretion disc (Ross & Fabian 1993), and consist of fluorescent and recombination emission lines as well as absorption features. In the inner regions of an accretion disc, the various reflection features become highly distorted due to relativistic effects and Doppler shifts. The shape of the prominent Fe-Kα fluorescent line, and more importantly the extent of its red wing, can give a direct indication of the radius of the reflecting material from the black hole (Fabian et al. 1989; Laor 1991; Fabian et al. 2000). The stable circular orbit around a black hole extends down to the radius of marginal stability, $r_{\rm ms}$, which depends on the spin parameter (e.g Bardeen, Press & Teukolsky 1972). A major advantage of using reflection features to obtain the spin of the black hole is that these features are completely independent of black hole mass and distance and can thus be used for any system where both or either of these parameters are unknown (for a review, see Miller 2007). For GX 339−4, we found that for both the very high and the low-hard state (LHS) the accretion disc extends to the innermost stable circular orbit (ISCO), $r_{\rm ms}$ at a radius of $\approx 2.05 r_{\rm g}$, where $r_{\rm g} = GM/c^2$ (Miller et al. 2008a; Reis et al. 2008). This implies a spin of $\approx$0.935 for GX 339−4.

In this paper, we use the method adopted by Reis et al. (2008) which uses a specially developed spectral grid, REFHIDEN (Ross & Fabian 2007), to obtain the spin parameter of SWIFT J1753.5−0127 and GRO J1655−40. J1753.5−0127 was first detected in hard

⋆E-mail: rcr36@ast.cam.ac.uk

X-rays by the Burst Alert Telescope (BAT) on the *SWIFT* satellite on 2005 May 30 (Palmer et al. 2005). Using *RXTE* and *XMM–Newton* data, Miller, Homan & Miniutti (2006, hereafter M06) showed the presence of a cool ($kT \approx 0.2$ keV) accretion disc extending close to the $r_{\rm ms}$ in the LHS of the system. The presence of this cool accretion disc was later confirmed by Ramadevi & Seetha (2007) and more recently by Soleri et al. (2008) using multiwavelength observations of the source.

GRO J1655−40 was discovered by the Burst And Transient Source Experiment (BATSE) on board of the Compton Gamma Ray Observatory (CGRO) on 1994 July 27 (Zhang et al. 1994). The mass of the compact object has been dynamically constrained to $>6.0\,{\rm M}_{\odot}$ (Orosz & Bailyn 1997). The *ASCA* observation of J1655−40 from 1994 through 1996 provided the first clear detection of absorption-line features in the source (Ueda et al. 1998; see also Miller et al. 2008b). Using archival *ASCA* data, Miller et al. (2006) showed evidence of highly skewed, relativistic lines and suggested an inner radius of reflection of $\approx 1.4 r_{\rm g}$ which would indicate a rapidly spinning black hole. This was later confirmed by Díaz Trigo et al. (2007, hereafter DT07) using simultaneous *XMM–Newton* and *INTEGRAL* observations of J1655−40 during the 2005 outburst. The high spin suggested by these authors is in contrast with the spin parameter reported by Shafee et al. (2006) of 0.65–0.75 using the thermal continuum method. In the following section, we detail the observation, analyses procedure and results.

2 OBSERVATION AND DATA REDUCTION

SWIFT J1753.5−0127 was observed in its LHS by *XMM–Newton* for 42 ks, starting on 2006 March 24 16:00:31 UT and simultaneously by *RXTE* for 2.3 ks starting at 17:26:06 UT (M06). The *EPIC*-pn camera (Struder et al. 2001) was operated in 'timing' mode with a 'medium' optical blocking filter. For GRO J1655−40, observations were made by *XMM–Newton* for 23.9 ks on 2005 March 18 15:47:13 (hereafter Obs 1) and again on 2005 March 27 08:43:59 (hereafter Obs 2) for 22.3 ks (DT07). The source was found to be in the high-soft state and was observed with the *EPIC*-pn camera in 'burst' mode with a 'thin' optical blocking filter. Starting with the unscreened level 1 data files for all aforementioned observation we extracted spectral data using the latest *XMM–Newton Science Analyses System v* 7.1.0 (SAS). For J1753.5−0127, events were extracted in a stripe in RAWX (20–56) and the full RAWY range. RAWX 30–43 and RAWY 5–160 was used for J1655−40. For both sources, bad pixels and events too close to chip edges were ignored by requiring 'FLAG = 0' and 'PATTERN ≤ 4'. The energy channels were grouped by a factor of 5 to create a spectrum. Background spectra were extracted for both sources from an adjacent region of similar RAWY and RAWX. In the case of J1655−40, the background is negligible due to the high source flux and it was not used for the analyses that follows. In both cases, individual response files were created using the SAS tools RMFGEN and ARFGEN. The *EPIC*-pn resulted in a total good-exposure time of 40.1 ks for J1753.5−0127. Due to the low duty cycle of the 'burst' mode (3 per cent), the total good exposure time for J1655−40 is ≈0.7 and 0.6 ks for Obs 1 and 2, respectively. *RXTE* data for J1753.5−0127 were reduced in the standard way using the HEASOFT v 6.0 software package. We used the 'Standard 2 mode' data from PCU-2 only. Standard screening resulted in a net Proportional Counter Array (PCA) and High-Energy X-ray Timing Experiment (HEXTE) exposures of 2.3 and 0.8 ks, respectively. To account for residual uncertainties in the calibration of PCU-2, we added 0.6 per cent systematic error to all energy channels. The *HEXTE-B* cluster was operated in the 'standard archive mode'. The FTOOL GRPPHA was used to give at least 20 counts per spectral bin.

We restrict our spectral analyses of the *XMM–Newton EPIC*-pn data for J1753.5−0127 to the 0.7–10.0 keV band. For J1655−40, we use 0.7–9.0 keV due to the uncertain calibration above 9.0 keV for the *EPIC*-pn burst mode. The PCU-2 and HEXTE spectrum are restricted to 5.0–25.0 and 20.0–100.0 keV band, respectively. A Gaussian line at 2.2–2.3 keV is introduced when fitting the *EPIC*-pn spectrum due to the presence of an instrumental feature in this energy range that resembles an emission line. This feature is likely to be caused by Au M-shell edges and Si features in the detector. All parameters in fits involving different instruments were tied and a normalization constant was introduced. XSPEC v 12.4.0 (Arnaud 1996) was used to analyse all spectra. The quoted errors on the derived model parameters correspond to a 90 per cent confidence level for one parameter of interest ($\Delta\chi^2 = 2.71$ criterion).

3 ANALYSIS AND RESULTS

Fig. 1 shows the data/model ratio for J1753.5−0127 fitted with a simple absorbed power-law (PHABS model in XSPEC with $N_{\rm H}$ fixed at 1.72×10^{21} cm^{-2}) in the energy range 2.5–5.0 and 8.0–10.0 keV and then extended to the full energy range. As first noted by M06 and more recently confirmed by Soleri et al. (2008), J1753.5−0127 shows clear indications of the presence of a cool accretion disc with a temperature of ≈0.2 keV in its LHS. The presence of an excess at ∼ 6.9 keV is indicative of Fe-Kα emission. Similarly for J1655−40, we fit the 0.7–4.0 and 7.0–9.0 keV energy range with a power law and a further multicolor disc blackbody (MCD; Mitsuda et al. 1984) modified by absorption in the interstellar medium. The value of $N_{\rm H}$ was kept constant for the two observations. The data/model ratio for J1655−40 extended to the full energy range is shown in Fig. 2. The presence of a broad Fe-Kα line emission extending to just over 3.0 keV as well as absorption features are clearly seen. Fitting the LHS of J1753.5−0127 with a simple absorbed power-law results in an unacceptable fit (Table 1) with various residuals in both the soft and the Fe-Kα energy range.

The presence of a soft disc excess and broad Fe-Kα emission line is usually modelled phenomenologically with a combination of a multicolor disc component such as DISKBB (Mitsuda et al. 1984) and a relativistic line such as the LAOR line profile (Laor 1991). This combination of components can give robust spin measurements

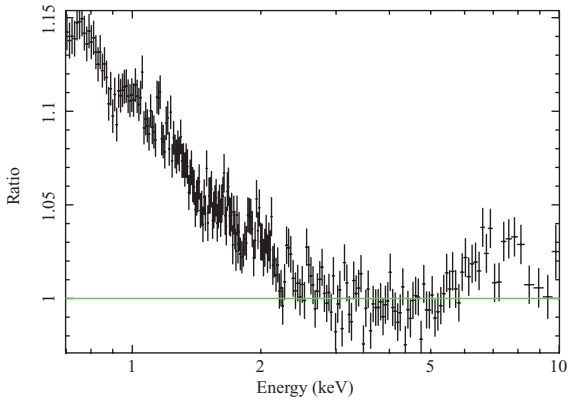

Figure 1. Data/model ratio for J1753.5−0127 obtained by fitting the energy range 2.5–5.0 and 8.0–10.0 keV with an absorbed power law. It is clear that a semiblackbody component as well as an iron reflection signature is present in the LHS of J1753.5−0127. The data have been rebinned for plotting purposes only.

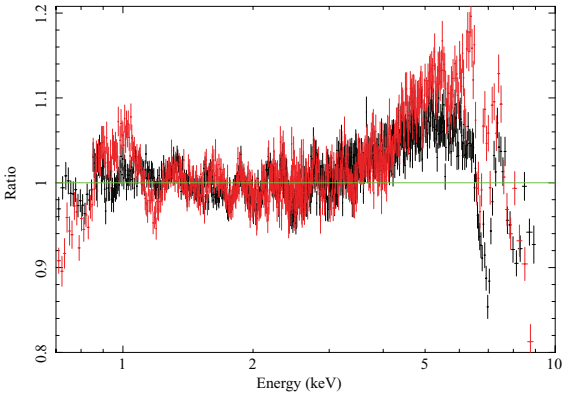

Figure 2. Data/model ratio for J1655−40 using a simple absorbed power law and disc blackbody fitted in the energy range 0.7–4.0 and 7.0–9.0 keV. Obs 1 and 2 are shown in black and red, respectively. The presence of a broad Fe-Kα line and complex absorption is clearly seen. The data have been rebinned for plotting purposes only.

Table 1. Results of fits to *XMM–Newton EPIC*-pn data for J1753.5−0127 with both a simple absorbed power law and the self-consistent reflection model REFHIDEN.

Parameter	Simple	REFHIDEN
$N_{\rm H}$ (10^{21} cm^{-2})	1.54 ± 0.13	$1.52^{+0.02}_{-0.03}$
Γ	1.631 ± 0.003	$1.54^{+0.01}_{-0.04}$
$N_{\rm PL}$	0.0591 ± 0.0002	$0.050^{+0.003}_{-0.004}$
kT (keV)		$0.193^{+0.003}_{-0.002}$
$H_{\rm den}$ ($\times 10^{20}$ H cm^{-3})		$1.40^{+0.13}_{-0.27}$
$R_{\rm illum/BB}$		$9.6^{+0.4}_{-0.6}$
$N_{\rm REFHIDEN}$		$0.0013^{+0.0004}_{-0.0006}$
$q_{\rm in}$		4^{+6}_{-1}
$r_{\rm in}(r_{\rm g})$		$3.1^{+0.7}_{-0.6}$
i (deg)		55^{+2}_{-7}
χ^2/ν	2191 .9/1859	1839.5/1852

Note. The self-consistent model is described in XSPEC as PHABS×KDBLUR×(PL+REFHIDEN). The normalization of each component is referred to as N. All errors refer to the 90 per cent confidence range for a single parameter.

when the presence of the Fe-Kα emission line is significantly above the continuum. However, it should be noted that it is only an approximation since the identification of $r_{\rm in}$, as determined from LAOR assumes a hard wired spin parameter of $a = 0.998$. Furthermore, the LAOR line profile is a phenomenological model for a relativistic *emission line*. The effects that extreme gravity have on the reflection signatures are not limited to the Fe-Kα line profile and thus a more thorough method to constrain the spin would involve modelling all of the reflection signatures present in the spectra. In what follows, we use the reflection model developed by Ross & Fabian (2007; REFHIDEN) to model all the reflection signatures as well as the disc blackbody emission in a self-consistent manner. This approach was detailed in Reis et al. (2008) for the Galactic black hole GX 339−4.

The reflection features produced by the illuminated surface layer of an accretion disc are largely dependent on the ionization state of the disc, and thus an important quantity is the ionization parameter $\xi = 4\pi F_{\rm h}/H_{\rm den}$, where $F_{\rm h}$ is the hard X-ray flux illuminating a disc with a hydrogen density $H_{\rm den}$ (Matt, Fabian & Ross 1993). The REFHIDEN reflection model incorporates the importance of the thermal emission from the disc midplane in determining the ionization state and thus reflection features. Whereas previous reflection models such as the constant-density ionized disc (CDID; Ballantyne, Ross & Fabian 2001) and REFLIONX (Ross & Fabian 2005) vary over the ionization parameter ξ and does not account for thermal emission, in REFHIDEN both the number density of hydrogen, $H_{\rm den}$, and the ratio of the total flux illuminating the disc to the total blackbody flux emitted by the disc ($R_{\rm illum/BB}$) are implicit parameters. The value of kT for the blackbody entering the surface layer from below and the power-law photon index are further parameters in the model. The disc reflection spectra are convolved with relativistic blurring kernel KDBLUR, which is derived from the code by Laor (1991). The parameters for the blurring kernel are the emissivity index $q_{\rm in}$, where the emissivity (ϵ_r) is described by a power-law profile such that $\epsilon_r = r^{-q_{\rm in}}$, disc inclination i, the inner disc radius $r_{\rm in}$ and the outer disc radius which was fixed at $400r_{\rm g}$. The power-law index of REFHIDEN is the same as that of the hard component.

3.1 Self-consistent reflection and disc emission

3.1.1 ***SWIFT J1753.5-0127***

The model provides an excellent fit to the data for J1753.5−0127 with $\chi^2/\nu = 1839.5/1852$. Table 1 details the parameter values with all errors corresponding to the 90 per cent confidence range. The data/model spectrum is shown in Fig. 3(a) with the fit extended to 100.0 keV using *RXTE* data shown in the inset. A normalization constant was added to account for flux mismatch between the instruments. The best-fitting model prior to gravitational blurring is shown in Fig. 3(b). The value of the inner radius obtained from the gravitational blurring of the reflection features is constrained to be $r_{\rm in} = 3.1^{+0.7}_{-0.6}\ r_{\rm g}$. The strong constraint on the value of $r_{\rm in}$ can be better appreciated in Fig. 4(a) , where the 90 per cent confidence level is shown in the χ^2 plot obtained with the 'steppar' command in XSPEC. Fig. 4(b) shows a similar constraint obtained for the inner accretion disc inclination of J1753.5−0127.

As can be seen from Table 1, the value of the emissivity index, $q_{\rm in}$, has been poorly constrained. A value of 3 is expected for a standard accretion disc (Reynolds & Nowak 2003) with steeper values usually being interpreted as emission from a small, compact, centrally located X-ray source, such as expected from the base of a jet (Miniutti & Fabian 2004). In order to investigate any degeneracy between the value of the inner radius and the unconstrained emissivity, we explored their parameter space using the 'contour' command in XSPEC. All parameters except for Γ and $R_{\rm illum/BB}$ were free to vary. Fig. 5(a) shows the 68, 90 and 95 per cent contour for two parameters of interest. Although the emissivity index is poorly constrained, it can be seen from Fig. 5(a) that the value of the inner radius is not strongly affected by this uncertainty. In what follows, we will thus freeze the value of the emissivity at the best-fitting value shown in Table 1. Figs 5(b) and (c) show similar contour plots for both inclination and $H_{\rm den}$ versus inner radius, respectively. For a large range of inclination and $H_{\rm den}$, the value of $r_{\rm in}$ remains approximately between 2 and $4r_{\rm g}$ with a best-fitting value of approximately $3r_{\rm g}$, in accordance to that shown in Fig. 4(a). Assuming that $r_{\rm in} = 3.1^{+0.7}_{-0.6}\ r_{\rm g}$ (Fig. 4a) is the same as the radius of marginal stability $r_{\rm ms}$, we obtain a dimensionless spin parameter of $0.76^{+0.11}_{-0.15}$ for J1753.5−0127 in its LHS (Fig. 6).

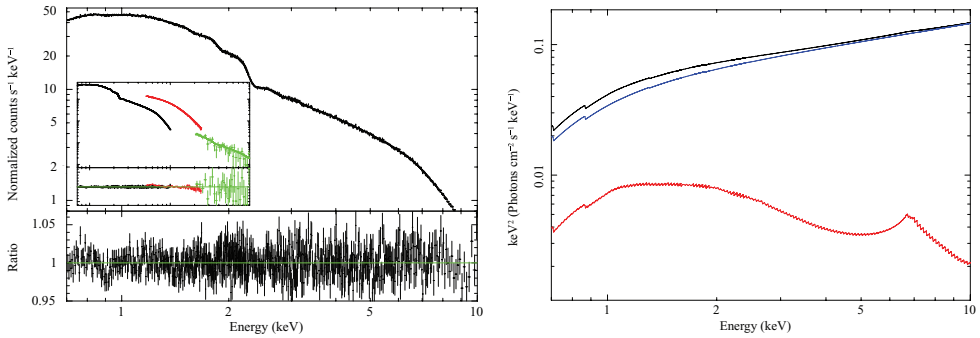

Figure 3. (a) Data/model ratio for J1753.5−0127 in its LHS. The model assumes a power-law emissivity profile and constitutes of a power-law and the disc reflection model REFHIDEN. The inset shows the model extended to 100.0 keV using *RXTE* PCA (red) and HEXTE (green). Data have been rebinned for plotting purposes only. (b) Best-fitting model prior to gravitational blurring showing the reflection features. The total model, power-law and reflection components are shown in black, blue and red, respectively.

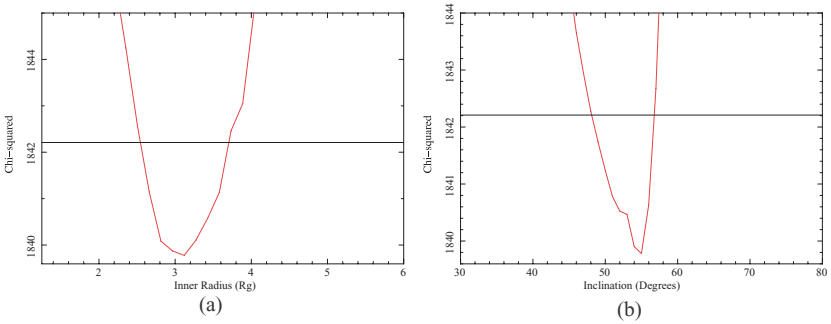

Figure 4. Panel (a): χ^2 versus $r_{\rm in}$ plot for J1753.5−0127. A value of $r_{\rm in} = 3.1^{+0.7}_{-0.6} r_{\rm g}$ is found at the 90 per cent confidence level for one parameter of interest ($\Delta\chi^2 = 2.71$ criterion) shown by the solid horizontal line. Panel (b): similar plot for the disc inclination. A value for the disc inclination of 55^{+2}_{-7} is found at the 90 per cent confidence level for one parameter of interest.

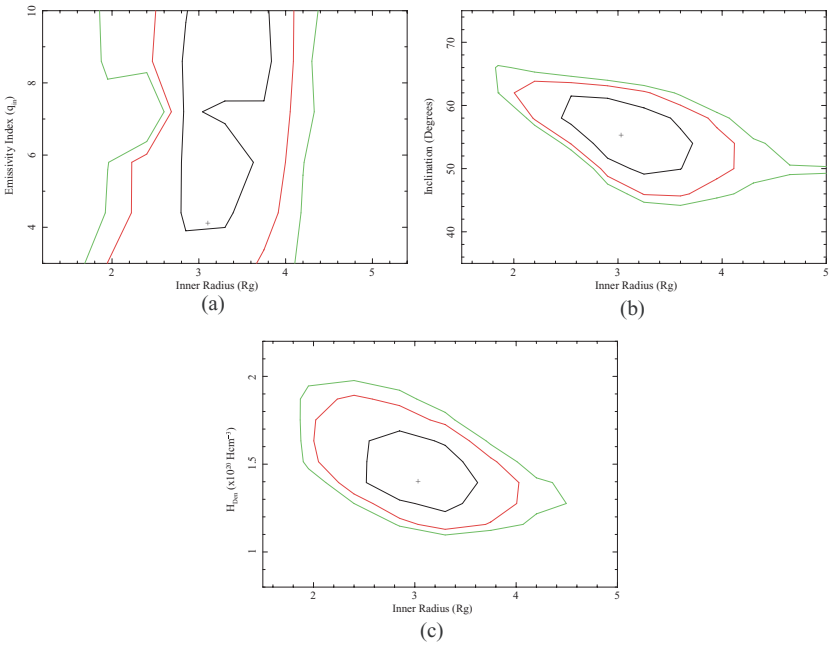

Figure 5. Panel (a): emissivity versus inner radius contour plot for J1753.5−0127. The 68, 90 and 95 per cent confidence range for two parameters of interest are shown in black, red and green, respectively. Panel (b): similar plot for the inclination versus inner radius. (c): hydrogen density versus inner radius. It can be seen that for the full range of the emissivity, inclination and hydrogen density, the inner radius is constrained between approximately 2–4$r_{\rm g}$ at the 90 per cent confidence level for two parameters.

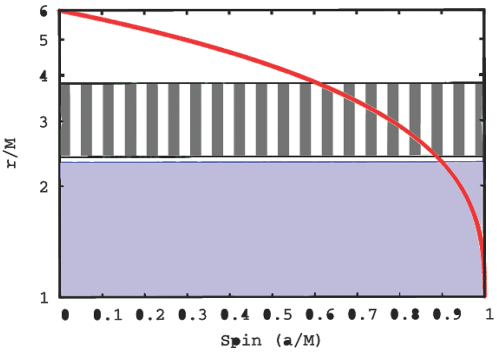

Figure 6. Plot of the ISCO versus dimensionless spin parameter (solid curve). The constraints imposed by the innermost radius obtained for J1753.5−0127 are shown by the intersection of the solid line with the vertical region. The solid region shows similar constrains for the lower limit of the spin parameter in J1655−40. Based on this analysis, a dimensionless spin parameters of $0.76^{+0.11}_{-0.15}$ is found for J1753.5−0127 and a lower limit of ≈0.90 is found for J1655−40.

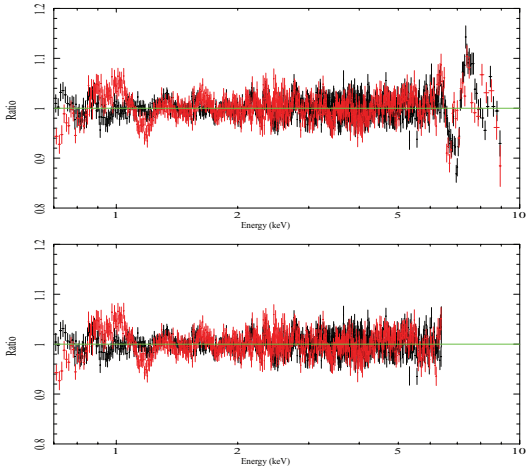

Figure 7. Top panel: best-fitting data/model ratio for J1655−40 using Model 1 (Table 2). The various absorption features are clearly seen. Bottom panel: similar as above for Model 2 covering the energy range 0.7–6.4 keV. The model clearly results in a good fit for the red wing of the Fe-Kα fluorescent line. Obs 1 and 2 are shown in black and red, respectively. The data have been rebinned for plotting purposes only.

3.1.2 *GRO J1655-40*

Strong absorption features are clearly present in the spectra of J1655−40 (see Fig. 2), and thus a fit with REFHIDEN should not immediately give an acceptable result. Fig. 7 (top panel) shows the best-fitting data/model ratio using REFHIDEN. The various parameters for this model are described in Table 2 (Model 1). It can be seen that, whereas in Fig. 2 there is evidence of both a broad line and various absorption features, this time the presence of the broad line has diminished (Fig. 7, top panel). This fit constrains the inner radius to $r_{\rm in} = 1.86^{+0.20}_{-0.02}\,r_{\rm g}$ with $\chi^2/\nu = 4967.3/3296$. The best fit using Model 1 seems to imply a relatively low inclination of $50^\circ \pm 1^\circ$, considerably less than the value of the binary inclination of $70.2^\circ \pm 1.9^\circ$ (Greene, Bailyn & Orosz 2001). However, this value is still in agreement with that presented by DT07 (see their table 1). The low inclination seen here could be due to the various

Table 2. Results of fits to *XMM–Newton EPIC*-pn data for J1655−40 with self-consistent reflection model REFHIDEN.

Parameter	Model 1		Model 2		Model 3		Model 4	
	Obs 1	Obs 2	Obs 1	Obs 2	Obs 1	Obs 2	Obs 1	Obs 2
$N_{\rm H}$	$0.76^{+0.01}_{-0.02}$	–	0.759 ± 0.001	–	0.765 ± 0.001	–	$0.742^{+0.004}_{-0.002}$	–
Γ	$2.59^{+0.03}_{-0.01}$	$2.88^{+0.03}_{-0.02}$	2.72 ± 0.08	$2.91^{+0.04}_{-0.053}$	$2.54^{+0.02}_{-0.01}$	$2.99^{+0.01}_{-0.02}$	$2.54^{+0.06}_{-0.02}$	$2.69^{+0.03}_{-0.02}$
$N_{\rm PL}$	$10.3^{+0.2}_{-0.4}$	$10.4^{+0.3}_{-0.1}$	$9.0^{+0.1}_{-0.2}$	11 ± 3	$10.4^{+0.1}_{-0.2}$	$9.46^{+0.23}_{-0.02}$	$8.18^{+0.16}_{-0.12}$	$9.35^{+0.14}_{-0.06}$
kT (keV)	$0.846^{+0.002}_{-0.007}$	0.84 ± 0.01	0.778 ± 0.009	$0.848^{+0.003}_{-0.002}$	$0.776^{+0.002}_{-0.008}$	$0.780^{+0.009}_{-0.001}$	0.804 ± 0.004	$0.816^{+0.007}_{-0.006}$
$H_{\rm den}$	$9.97^{+0.03}_{-0.56}$	$10^{+0.0}_{-0.2}$	$9.0^{+0.3}_{-0.7}$	8^{+1}_{-2}	$7.4^{+0.3}_{-0.1}$	10^{+0}_{-1}	$10.0^{+0.0}_{-0.6}$	$9.0^{+0.7}_{-0.6}$
$R_{\rm illum/BB}$	$0.93^{+0.02}_{-0.04}$	$0.20^{+0.03}_{-0.01}$	$0.39^{+0.05}_{-0.10}$	0.6 ± 0.2	$0.11^{+0.01}_{-0.03}$	$0.01^{+0.20}$	$1.0^{+0.03}_{-0.02}$	$0.169^{+0.074}_{-0.007}$
$N_{\rm ref}$	$3.3^{+0.4}_{-0.2}$	$0.29^{+0.06}_{-0.09}$	$1.4^{+0.1}_{-0.3}$	0.7 ± 0.2	$0.46^{+0.31}_{-0.02}$	$0.02^{+0.10}$	$3.42^{+0.01}_{-0.04}$	$0.251^{+0.002}_{-0.007}$
$q_{\rm in}$	$10.0_{-0.3}$	4.5 ± 0.1	$10.0^{+0.0}_{-0.3}$	$10.0^{+0.0}_{-0.5}$	$10.0^{+0.0}_{-0.4}$	$7.75^{+0.06}_{-0.20}$	3.87 ± 0.08	$2.75^{+0.03}_{-0.02}$
$r_{\rm in}(r_{\rm g})$	$1.86^{+0.20}_{-0.02}$	–	1.31 ± 0.01	–	1.38 ± 0.01	–	$2.17^{+0.15}_{-0.17}$	–
i	50 ± 1	–	70(f)	–	70(f)	–	30^{+5}_{-10}	–
$E_{\rm GABS1}$ (keV)	–	–	–	–	6.7(f)	6.7(f)	6.7(f)	6.7(f)
σ(keV)	–	–	–	–	0.08 ± 0.02	0.003 ± 0.001	0.09 ± 0.03	0.004 ± 0.001
τ	–	–	–	–	$0.030^{+0.003}_{-0.005}$	0.20 ± 0.06	$0.031^{+0.006}_{-0.005}$	$0.22^{+0.08}_{-0.07}$
$E_{\rm EDGE1}$ (keV)	–	–	–	–	8.8(f)	8.8(f)	8.8(f)	8.8(f)
$E_{\rm GABS2}$ (keV)	–	–	–	–	6.97(f)	6.97(f)	6.97(f)	6.97(f)
σ(keV)	–	–	–	–	0.06 ± 0.02	<0.8	$0.056^{+0.019}_{-0.020}$	<0.05
τ	–	–	–	–	$0.041^{+0.004}_{-0.005}$	$0.014^{+0.016}_{-0.008}$	$0.039^{+0.005}_{-0.002}$	$0.013^{+0.023}_{-0.005}$
$E_{\rm EDGE2}$ (keV)	–	–	–	–	9.3(f)	9.3(f)	9.3(f)	9.3(f)
χ^2/ν	4967.3/3296	–	3230.0/2264	–	4425.3/3289	–	4370.1/3288	

Note. Model 1 is described in XSPEC as PHABS×KDBLUR×(PL+REFHIDEN). The value of $N_{\rm H}$, inclination and $r_{\rm in}$ were tied between the two observations. An instrumental line at 1.876 keV was added to each model. The normalization of each component is referred to as N. Frozen values are followed by (f). $H_{\rm den}$ is given in units of 10^{21} H cm^{-3}. $N_{\rm H}$ is given in units of 10^{22} cm^{-2}. Model 2 is similar to the previous model and only fitted to the data below 6.6 keV. Models 3 and 4 include Fe XXV and Fe XXVI absorptions (GABS model in XSPEC) at fixed energies of 6.7 and 6.97 keV, respectively. Their respective absorption edges are modelled with the model EDGE in XSPEC with energies frozen at 8.8 and 9.3 keV, respectively. The optical depth τ of the absorptions and edges are linked for consistency.

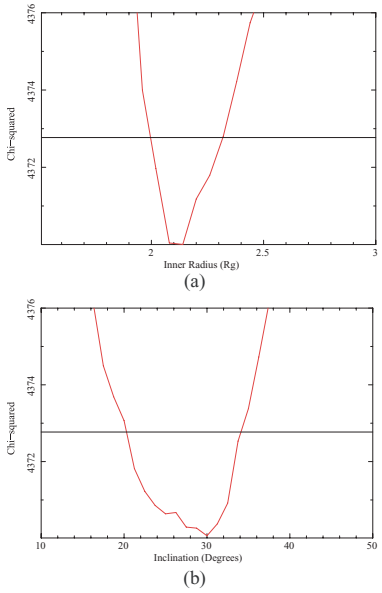

Figure 8. Panel (a): χ^2 versus $r_{\rm in}$ plot for J1655−40. Using Model 4 (Table 2) with the inclination allowed to vary over its full range we obtain a value of $2.17^{+0.15}_{-0.17}\,r_{\rm g}$ for the inner radius at the 90 per cent confidence level for one parameter of interest ($\Delta\chi^2 = 2.71$ criterion) shown by the solid horizontal line. Panel (b): similar plot for the inclination of J1655−40.

absorption features masking themselves as the blue wing of an Fe-Kα line profile.[1] Although various features contribute to the determination of the inner radius of emission and thus spin of the black hole, the most important of those features for the purpose of this work is the extent of the red wing in the Fe-Kα fluorescent line. In order to explore whether the absorption features are affecting the value of the inner radius, we froze the inclination at 70° and modelled the spectra below 6.4 keV. The results of this fit is detailed in Model 2 (Table 2) and shown in Fig. 7 (bottom panel). By restricting the inclination to the known value of the binary inclination (≈70°) and fitting the spectra below 6.4 keV, the innermost radius approaches that of a maximally rotating black hole with $r_{\rm in} = 1.31 \pm 0.01 r_{\rm g}$ and $\chi^2/\nu = 3230.0/2264$. The majority of the contribution to χ^2 is now coming from residuals between 0.9 and 1.1 keV possibly due to the photoionization edge of O VIII at ≈0.9 keV. In order to extend this fit to the full range, we modelled the various absorption features in a phenomenological manner using two negative Gaussian absorptions (GABS model in XSPEC) fixed at energies of 6.7 and 6.97 keV corresponding to absorption of helium-like Fe XXV and hydrogen-like Fe XXVI, respectively, as well as absorption edges fixed at 8.8 and 9.3 keV. The optical depths τ of the absorptions and edges were linked for self-consistency. The various parameters for this model covering the full energy range are detailed in Table 2 (Model 3). The value of the inner radius remains low ($<1.4 r_{\rm g}$) similar to that of Model 2. Allowing the inclination to vary over its full range improved the statistics with $\Delta\chi^2 = -55.2$ for 1 less degree of freedom (Model 4) and resulted in an inner radius of $r_{\rm in} = 2.17^{+0.15}_{-0.17} r_{\rm g}$ (Fig. 8a) and an inclination of $30^{\circ\,+5}_{-10}$ (Fig. 8b). The best-fitting spectra for J1655−40 including the absorption lines and edges are shown in Fig. 9. Note that as we remove the restriction on the inclination the emissivity profile of the two observations

[1] The blue wing of the Fe-Kα line profile can be used to determine the inclination of the source (see e.g. Reynolds & Nowak 2003; Fabian & Miniutti 2009).

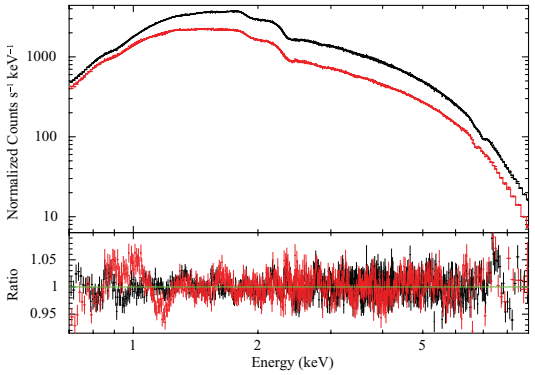

Figure 9. Best-fitting spectra for J1655−40 using Model 4. Obs 1 and 2 are shown in black and red, respectively. The complex absorptions are phenomenologically modelled with two Gaussian absorption (see the text). The data have been rebinned for plotting purposes only.

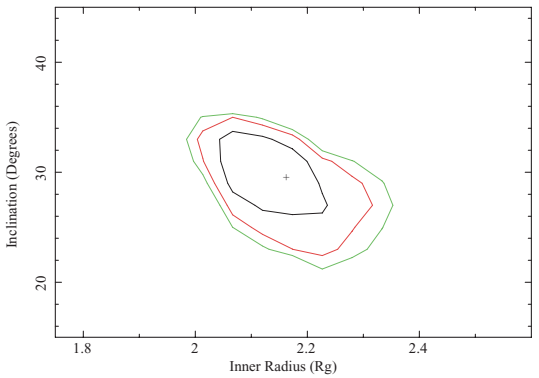

Figure 10. Inclination–inner-radius contour plot for J1655−40. The 68, 90 and 95 per cent confidence range for two parameters of interest are shown in black, red and green, respectively. It can be seen that for the inner radius is constrained to be below approximately $2.5 r_{\rm g}$ for a large range of inclination at the 90 per cent confidence level for two parameters.

becomes less steep, with the indices constrained to $q_{\rm in} = 3.87 \pm 0.08$ and $2.75^{+0.03}_{-0.02}$ for observations 1 and 2, respectively. Adding a possible nickel emission line at 7.48 keV with equivalent width of 30 and 17 ev for obs 1 and 2, respectively, resulted in an improved fit with $\Delta\chi^2 = -72.2$ for 4 extra degrees of freedom. As was the case for Model 2, most of the contribution to chi-squared is now coming from residuals in the soft energy range. By restricting this fit to above 1.5 keV, we obtain $\chi^2/\nu = 3496.0/2957$.

Similar to J1753.5−0127, we investigate any degeneracy between the inclination and inner radius in Model 4 by using the 'contour' command in XSPEC. All parameters except for Γ and $R_{\rm illum/BB}$ were free to vary. Fig. 10 shows the 68, 90 and 95 per cent contour for the two parameters of interest. It can be seem from Fig. 10 that for a large range of inclination the value of $r_{\rm in}$ remains below $2.35 r_{\rm g}$ with a best-fitting value of approximately $2.15 r_{\rm g}$, in agreement with the result presented in Fig. 8a. It is clear that the unknown inclination of the system plays an important role in the determination of the inner radius (and thus spin) of J1655−40, with values as low as $1.3 r_{\rm g}$ (spin > 0.99) obtained with an inclination of 70° (Model 2) rising to $2.32 r_{\rm g}$ (spin > 0.9) with the inclination allowed to vary (Model 4). However, it must be noted that using the reflection model both with and without accounting for the absorption features as well as both with and without constraints on the inclination gives results with an inner radius consistently below $2.32 r_{\rm g}$ (Table 2). Taking

this value as an upper limit to the innermost radius of emission implies a dimensionless spin parameter greater than 0.9 for J1655−40 (Fig. 6).

4 DISCUSSION

The X-ray spectra of galactic black hole binaries can provide important information on both the geometry of the system and intrinsic physical parameters such as the spin of the central black hole. Using the reflection features embedded in the spectra of both J1753.5−0127 and J1655−40, we found clear indications that the accretion disc extends close to the radius of marginal stability in both cases. For J1753.5−0127, we have shown that the innermost emitting region extends down to $r_{\rm in} = 3.1^{+0.7}_{-0.6} r_{\rm g}$ (Fig. 4a) with an innermost inclination of $55^{\circ}{}^{+2}_{-7}$ (Fig. 4b). Based on the normalization of the disc blackbody component, M06 found an inner radius of $r_{\rm in} = 2.0(3)(M/10\,{\rm M}_{\odot})(d/8.5\,{\rm kpc})(\cos i)^{-1/2} r_{\rm g}$, similar to ours for a large range of parameters. Our result is also consistent with that found by Soleri et al. (2008) of 2.6–6.0$r_{\rm g}$ for a $10\,{\rm M}_{\odot}$ black hole. In both these cases, $r_{\rm in}$ was estimated using the normalization of the MCD component and thus requires knowledge of the mass, distance and inclination of the sources. Uncertainties in these values can significantly affect the value of the inner radius and thus spin parameter.

Estimating the spin of a black hole based on the extent of the emitting region relies on the assumption that the accretion disc extends to the ISCO and that emission within this radius is negligible. Reynolds & Fabian (2008) addressed the robustness of this assumption and found that reflection within the ISCO becomes significantly less as one considers more rapidly rotating black holes. The way the dimensionless spin parameter depends on the position of the ISCO is shown in Fig. 6 (solid curve). Assuming that the accretion disc extend to the ISCO for J1753.5−0127, we obtain a spin parameters of $0.76^{+0.11}_{-0.15}$. Note that this estimate is independent of the unknown distance to the source.

The system in J1655−40 is known to have an orbital plane inclination of approximately 70° (Greene et al. 2001). Constraining the inclination to this value resulted in an inner radius of emission consistent with that of a maximally rotating black hole (Model 3; Table 2). Allowing the inclination of the blurring function to be a free parameter in the spectral fit of J1655−40, we obtain an improved fit with an inner radius of $=2.17^{+0.15}_{-0.17} r_{\rm g}$ (Fig. 8a) and an inner-disc inclination of $30^{\circ}{}^{+5}_{-10}$ (Fig. 8b). This value for the inner radius implies a *lower limit* for the spin parameter of 0.9 (Fig. 6a). The possibility of a misalignment between the innermost region of the accretion disc and the orbital plane inclination in galactic microquasars has been suggested by various authors (see e.g. Maccarone 2002) with clear examples seen in both J1655−40 (Martin, Tout & Pringle 2008b) and V4641 Sgr (Martin, Reis & Pringle 2008a). It was shown in Martin et al. (2008b) that the alignment time-scale in microquasar such as J1655−40 is usually a significant fraction of the lifetime of the system. Thus, if the black hole in such a system was formed with misaligned angular momentum, as expected from supernova-induced kicks, then it would be likely that the system would remain misaligned for most of its lifetime. This assumption is supported by the apparent misalignment found in this work.

The lower limit for the spin parameter of J1655−40 found here (>0.9; Fig. 6) is not consistent with that reported by Shafee et al. (2006) of 0.65–0.75. As was mentioned above, their method requires prior knowledge of several other factors including the inner-disc inclination and distance to the source. Pszota & Cui (2007) have recently shown that neither disc continuum models KERRBB (Li et al. 2005) nor BHSPEC (Davis & Hubeny 2006) were able to successfully model the ultrasoft spectra of GX 339−4, nonetheless their best-fitting parameters in conjunction with the best estimates for the physical parameters of the source suggested a moderate spin of 0.5–0.6 in comparison with our estimate of ≈0.935 (Miller et al. 2008a; Reis et al. 2008) based on the various reflection features in the spectra of GX 339−4. Our suggestion that J1655−40 contains a rapidly rotating black hole is in agreement with results based on quasi-periodic oscillations where a value of >0.91 is usually derived (Zhang, Cui & Chen 1997; Cui, Zhang & Chen 1998; Wagoner, Silbergleit & Ortega-Rodríguez 2001; Rezzolla et al. 2003). Furthermore, in their derivation of the spin parameter of J1655−40, Shafee et al. (2006) assumed both a lack of misalignment between the central disc region and the orbital plane and more importantly they used a distance to the source of 3.2 ± 0.2 kpc. Foellmi (2008) has recently shown that the distance to J1655−40 is most likely to be less than 2 kpc. When this distance is used in place of 3.2 kpc, the spin parameter of J1655−40 derived by the thermal continuum method becomes greater than 0.91 in agreement with our results.

5 CONCLUSIONS

We have studied the *XMM–Newton* spectra of both SWIFT J1753.5−0127 and GRO J1655−40. By estimating the innermost radius of emission in these systems, we constrain their spin parameters by assuming that the accretion disc extends down to the radius of marginal stability. For J1753.5−0127, the spin is found to be $0.76^{+0.11}_{-0.15}$ at 90 per cent confidence. The innermost disc inclination in J1753.5−0127 is estimated at $55^{\circ}{}^{+2}_{-7}$. In the case of J1655−40, we find that the best fit requires a disc which is significantly misaligned to the orbital plane. An inclination of $30^{\circ}{}^{+5}_{-10}$ and a dimensionless spin parameter greater than 0.9 are found at the 90 per cent confidence level. Our method involves spectral modelling of both the intrinsic disc thermal emission and the reprocessed hard radiation which manifest itself as various reflection 'signatures'. These reflection signatures are independent of both black hole mass and distance and are thus a very useful tool for such measurements.

ACKNOWLEDGMENTS

RCR acknowledges STFC for financial support. ACF and RRR thank the Royal Society and the College of the Holy Cross, respectively.

Note added after submission: Hiemstra et al. (2009) have analysed the same *XMM–Newton* and *RXTE* data for J1753.5−0127 used here. They independently confirm the existence of a broad Fe-Kα line and show that various continuum models with the addition of a LAOR line can successfully fit the data. More importantly, they claim to successfully fit the X-ray spectrum of J1753.5−0127 with a continuum model that does not require emission from a disc extending down to the ISCO. We have investigated this solution and find that in their case the broad line in a consequence of Compton broadening of the emitted photons by the hot surface of the accretion disc (Ross, Fabian & Young 1999; Ross & Fabian 2007). Their solution requires a highly ionized disc ($\xi \sim 5000\,{\rm erg\,cm\,s^{-1}}$) truncated at $\sim 255 r_{\rm g}$ with an inclination angle consistent with zero. Using the same reflection model (REFLION; Ross & Fabian 2005) convolved with KDBLUR and including a disc component, we find a further solution where the disc extends down to the ISCO ($6r_{\rm g}$) and has a much lower ionization parameter of $\xi \sim 500\,{\rm erg\,cm\,s^{-1}}$. This second interpretation yields an inclination

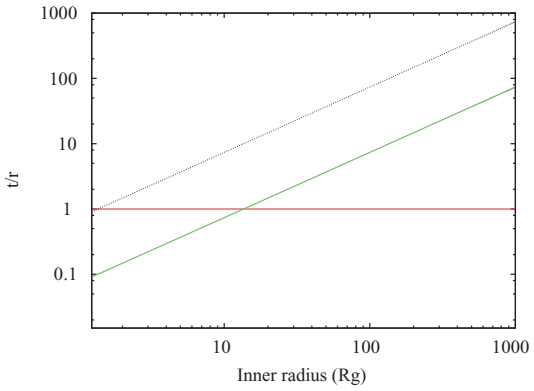

Figure 11. Ratio of half thickness t over inner radius r as a function of r for $\xi = 5000$ (dotted line) and $\xi = 500\,\mathrm{erg\,cm\,s^{-1}}$ (solid line). For a typical thin accretion disc, this ratio should be well below 1 (horizontal line).

of $\sim 65^\circ$ and an improvement of -7.7 in χ^2 for 2 extra degrees of freedom. The solution presented in our paper reflects that of the lower ionization reported above. We are concerned that in a solution with such high-ionization parameter and a truncation radius at $\sim$45 times the ISCO would result in a disc which is approximately 2×10^4 times less dense than that of a similar disc extending down to the ISCO. With an estimated mass of approximately $10\,\mathrm{M}_\odot$ (Cadolle Bel et al. 2007), a radius of $255 r_\mathrm{g}$ is the equivalent of a disc truncated at $\approx 3.8 \times 10^8$ cm from the central black hole. Using the ionization parameter and unabsorbed flux presented in Hiemstra et al. (2009), we can estimate the hydrogen number density to be approximately $2.3 \times 10^{15}\,\mathrm{cm^{-3}}$. A modest surface layer of Thomson depth $\tau_\mathrm{T} \sim 3$ will thus result in a disc with a half thickness, $t > 2 \times 10^9$ cm; at least five times larger than the truncation radius. For a disc with inner radius $r \gg r_\mathrm{g}$, we can write the ionization parameters as $\xi \approx 1.13 \times 10^5\ \eta\ t/r^2\ \mathrm{erg\,cm\,s^{-1}}$, where η is the X-ray efficiency (Reynolds & Begelman 1997). Fig. 11 shows the ratio t/r as a function of r for a system with $\eta = 0.06$ and an ionization parameter of 5000 and $500\,\mathrm{erg\,cm\,s^{-1}}$. For a typical thin accretion disc, t/r should be well below unity and as can be seen in Fig. 11; there are no solutions in this range for a disc with $\xi \sim 5000\,\mathrm{erg\,cm\,s^{-1}}$. We conclude that the high-ionization solution found by Hiemstra et al. (2009) is physically inconsistent; the disc must extend in to small radii.

REFERENCES

Arnaud K. A., 1996, in Jacoby G. H., Barnes J., eds, ASP Conf. Ser. Vol. 101, Astronomical Data Analysis Software and Systems V. Astron. Soc. Pac., San Froncisco, p. 17

Ballantyne D. R., Ross R. R., Fabian A. C., 2001, MNRAS, 327, 10

Bardeen J. M., Press W. H., Teukolsky S. A., 1972, ApJ, 178, 347

Cadolle Bel M. et al., 2007, ApJ, 659, 549C

Cui W., Zhang S. N., Chen W., 1998, ApJ, 493, L75

Davis S. W., Hubeny I., 2006, ApJS, 164, 530

Díaz Trigo M., Parmar A. N., Miller J., Kuulkers E., Caballero-García M. D., 2007, in Antonelli L. P. et al., eds, AIP Conf. Proc. Vol. 924, The Multicolored Landscape of Compact Objects and their Explosive Origins. Springer-Verlag, Berlin, p. 877

Fabian A. C., Miniutti G., 2009, in Wiltshire D. L., Visser M., Scott S. M., eds, The Kerr Spacetime: Rotating Black Holes in General Relativity. Cambridge Univ. Press, Cambridge, p. 236

Fabian A. C., Rees M. J., Stella L., White N. E., 1989, MNRAS, 238, 729

Fabian A. C., Iwasawa K., Reynolds C. S., Young A. J., 2000, PASP, 112, 1145

Foellmi C., 2008, New Astron., submitted (arXiv:0812.4232v2)

Greene J., Bailyn C. D., Orosz J. A., 2001, ApJ, 554, 1290

Hiemstra B., Soleri P., Mendez M., Belloni T., Mostafa R., Wijnands R., 2009, in press (arXiv:0901.225511)

Laor A., 1991, ApJ, 376, 90

Li L.-X., Zimmerman E. R., Narayan R., McClintock J. E., 2005, ApJS, 157, 335

Liu J., McClintock J. E., Narayan R., Davis S. W. and Orosz J. A., 2008, ApJ, 679, L37

Maccarone T. J., 2002, MNRAS, 336, 1371

McClintock J. E., Remillard R. A., 2006, in Lewin W. H. G., van der Klis M., eds, Compact Stellar X-ray Sources. Cambridge Univ. Press, Cambridge, p. 157

McClintock J. E., Shafee R., Narayan R., Remillard R. A., Davis S. W., Li L.-X., 2006, ApJ, 652, 539

Martin R. G., Reis R. C., Pringle J. E., 2008a, MNRAS, 391, 15

Martin R. G., Tout C. A., Pringle J. E., 2008b, MNRAS, 387, 188

Matt G., Fabian A. C., Ross R. R., 1993, MNRAS, 264, 839

Miller J. M., 2007, ARA&A, 45, 441

Miller J. M., Fabian A. C., Nowak M. A., Lewin W. H. G., 2006, in Novello M., Perez Bergliaffa S., eds, Proc. 10th Marcel Grossmann Meeting, Recent Developments in Theoretical and Experimental General Relativity, Gravitation and Relativistic Field Theories, Rio de Janeiro, Brazil. World Scientific Press, Singapore, p. 1296

Miller J. M., Homan J., Miniutti G., 2006, ApJ, 652, L113 (M06)

Miller J. M. et al., 2008a, ApJ, 679, L113

Miller J. M., Raymond J., Reynolds C. S., Fabian A. C., Kallman T. R., Homan J., 2008b, ApJ, 680, 1359

Miniutti G., Fabian A. C., 2004, MNRAS, 349, 1435

Mitsuda K. et al., 1984, PASJ, 36, 741

Orosz J. A., Bailyn C. D., 1997, ApJ, 477, 876

Palmer D. M., Barthelmey S. D., Cummings J. R., Gehrels N., Krimm H. A., Markwardt C. B., Sakamoto T., Tueller J., 2005, Astron. Telegram, 546

Pszota G., Cui W., 2007, ApJ, 663, 1206

Ramadevi M. C., Seetha S., 2007, MNRAS, 378, 182

Reis R. C., Fabian A. C., Ross R. R., Miniutti G., Miller J. M., Reynolds C., 2008, MNRAS, 387, 1489R

Reynolds C. S., Begelman M. C., 1997, ApJ, 488, 109

Reynolds C. S., Fabian A. C., 2008, ApJ, 675. 1048R

Reynolds C. S., Nowak M. A., 2003, Phys. Rep., 377, 389

Rezzolla L., Yoshida S., Maccarone T. J., Zanotti O., 2003, MNRAS, 334, L37

Ross R. R., Fabian A. C., 1993, MNRAS, 261, 74

Ross R. R., Fabian A. C., 2005, MNRAS, 358, 211

Ross R. R., Fabian A. C., 2007, MNRAS, 381, 1697

Ross R. R., Fabian A. C., Young A. J., 1999, MNRAS, 306, 461

Shafee R., McClintock J. E., Narayan R., Davis S. W., Li L.-X., Remillard R. A., 2006, ApJ, 636, L113

Soleri P. et al., 2008, in Bandyopadhyay R. M. Wachter S., Gelino D., Gelino C. R., eds, AIP Conf. Proc. Vol. 1010, A Population Explosion: The Nature & Evolution of X-ray Binaries in Diverse Environments. Springer-Verlag, Berlin, p. 103

Struder L. et al., 2001, A&A, 365, L18

Ueda Y., Inoue H., Tanaka Y., Ebisawa K., Nagase F., Kotani T., Gehrels N., 1998, ApJ, 492, 782

Wagoner R. V., Silbergleit A. S., Ortega-Rodríguez M., 2001, ApJ, 559L, 25

Zhang S. N., Cui W., Chen W., 1997, ApJ, 482, 155

Zhang S. N., Wilson C. A., Harmon B., Fishman G. J., Wilson R. B., Paciesas W. S., Scott M., Rubin B. C., 1994, IUA Circ. 6046

This paper has been typeset from a TEX/LATEX file prepared by the author.